Reduction of misfit dislocation density in metamorphic heterostructures by design optimization of the buffer layer with non-linear graded composition profile

© M.Yu. Chernov, V.A. Solov'ev, S.V. Ivanov

Ioffe Institute,
194021 St. Petersburg, Russia
E-mail: chernov@beam.ioffe.ru

Received April 26, 2023
Revised May 2, 2023
Accepted May 2, 2023

Equilibrium distributions of misfit dislocation density along the growth direction of metamorphic buffer layers $In_xAl_{1-x}As/GaAs$ with maximum In content $x_{max} \geq 0.77$ and different non-linear graded composition profiles $x \propto z^{1/n}$ are calculated. The effect of the initial In composition $(n = 2)$ of $In_xAl_{1-x}As$ buffer layer with convex-graded (x_{min}) composition profile on misfit dislocation density as well as amount of residual stresses at its top part is considered. Using computational approach, it was shown that a dislocation-free region is formed under thin tensile-strained GaAs layer $(1-10\,nm)$ inserted into InAlAs metamorphic buffer layer, which agrees with experimental data obtained early by transmission electron microscopy. Novel non-linear graded composition profile of metamorphic buffer layer has been proposed, which results in twice reduction of misfit dislocation density as compared to the convex-graded one. In addition, equilibrium distributions of misfit dislocation density in the HEMT heterostructures with two-dimensional electron channel $In_xAl_{1-x}As$, which are based on $In_{0.75}Ga_{0.25}As/In_{0.75}Al_{0.25}As$ metamorphic buffer layer of various designs, are calculated. The values of inverse steps (Δ), representing the difference between the maximum In content of $In_xAl_{1-x}As$ (x_{max}) and In content of $In_{0.75}Al_{0.25}As$ virtual substrate, at which relaxation of the elastic strains in 2D channel $In_{0.75}Ga_{0.25}As/In_{0.75}Al_{0.25}As$ doesn't occur, are calculated for metamorphic buffer layers $In_xAl_{1-x}As$ with convex-graded and optimized non-linear graded composition profiles.

Keywords: metamorphic heterostructures, metamorphic buffer layer, misfit dislocations, elastic stresses, In(Ga,Al)As/GaAs.

DOI: 10.21883/SC.2023.03.56230.4915

1. Introduction

Significant interest in the development of semiconductor devices of modern electronics based on $In_x(Ga,Al)_{1-x}As$ solid solutions with a high content of In $(x \geq 0.7)$, including high electron mobility transistors (HEMT) [1], heterojunction bipolar transistors [2], as well as semiconductor LEDs and lasers emitting in the mid-infrared range $(2-5\,\mu m)$ [3], has recently become stronger due to the opportunities of implementing such heterostructures on GaAs substrates, which are characterized by high manufacturability and low cost compared to traditionally used InAs, InSb and GaSb substrates. Meanwhile, the high density of misfit dislocations (MD) and the so-called threading dislocations (TD) that arise in heterostructures, due to a strong mismatch between the crystal lattice parameters of the GaAs substrate (a_s) and the active area (a) $\Delta a/a > 5\%$, has a negative effect on output parameters of device structures, and also leads to their degradation.

Over the past few years, various methods have been developed to obtain semiconductor heterostructures with an acceptable defect density on substrates that are strongly mismatched in the lattice parameter. In particular, such methods include substrate gluing (*wafer bonding*) [4], epitaxy on structured substrates (*patterned substrates*) [5], as well as metamorphic technology [3]. All approaches, except for the last one, include pretreatment of substrates using mechanical, chemical, and other methods before the start of epitaxial growth, which significantly complicates the implementation of heterostructures based on them; therefore, from a technological point of view, the metamorphic approach is more preferable.

The key element of the metamorphic technology is the metamorphic buffer layer (MBL). Since the 60s MBL with a composition gradient along the growth axis are widely used [6]. It was found that MBL with a monotonically varying composition contain in the upper part a region practically free from dislocations, with a thickness of d_{free}, in which residual elastic mechanical stresses accumulate [7]. Meanwhile, in the rest of the MBL, due to a strong mismatch between the lattice parameters of the substrate and the growing layer, the relaxation of elastic stresses occurs through the formation of a MD network. Residual stresses accumulated in the upper part of the MBL are usually compensated by the inverse step (Δ), which is the difference between the final composition of the MBL and the composition of the virtual substrate (VS) — layer grown on top of the MBL.

It should be noted that the distribution of the dislocation density over its thickness strongly depends on the choice of the MBL composition gradient. Nowadays metamorphic heterostructures traditionally use MBL with a linear [8,9]

or stepped [10,11] profile of composition change due to their relatively simple technological implementation. Nevertheless, according to several theoretical [12–14] and experimental papers [15,16], MBL with a nonlinear profile allow to obtain a dislocation-free area of greater thickness, as well as a lower dislocation density than MBL with a linear or stepped gradient. In particular, we have previously experimentally shown that the use of InAlAs MBLs with a root profile of composition change in In(As,Sb)/In(Ga,Al)As/GaAs metamorphic heterostructures allows to reduce the dislocation density by almost an order of magnitude compared to MBL with linear composition gradient [16]. However, the search for the optimal profile of changes in the composition of MBL in order to obtain metamorphic heterostructures based on it with the lowest potential density of defects remains an urgent task even today day.

This paper is devoted to optimizing the design of the $In_xAl_{1-x}As/GaAs$ ($x_{max} \geq 0.77$) MBL, including the profile and boundaries of composition change, by numerically simulating the MD density distribution as part of the energy model [17] along the direction of epitaxial growth of the MBL in order to achieve the minimum potential MD density in the upper part of the MBL and in the layers grown on top of it, as well as comparison of the calculation results with previously obtained experimental data. In addition, calculations were made of the equilibrium density distribution of MDs over the thickness of metamorphic HEMT heterostructures with a two-dimensional electron channel $In_{0.75}Ga_{0.25}As/In_{0.75}Al_{0.25}As$ containing MBL $In_xAl_{1-x}As$ of various designs.

2. Method of calculating the density distribution of misfit dislocations in MBL

The numerical method of calculation as part of the energy model is based on the iterative search for the minimum value of the system total energy [17]. MBL or a heterostructure based on it with a thickness of L are divided into$N$ sublayers. The total energy of the system, including the elastic energy (E_ε) and the MD energy (E_d) — the first and second terms in the formula (1), respectively, was calculated as follows:

$$E = \sum_{i=1}^{N} \varepsilon^2[i] \cdot Y[i] \cdot h + \sum_{i=1}^{N} K[i] \cdot \rho[i] \cdot h, \qquad (1)$$

where h — grid step, Y — Young's modulus, ρ — MD density, ε — elastic stresses, K — ratio expressed in terms of shear modulus, Poisson's ratio and Burgers vector in accordance with paper [17].

The essential parameters for the calculation, such as the lattice parameter, the length of the Burgers vector, elastic moduli, etc., were taken from [14]. The angle between the Burgers vector and the dislocation line (α) was assumed to be 60°, taking into account the fact that in heterostructures with a crystal lattice of the zinc blende type, the most characteristic MD are 60° dislocations. In all calculations of this paper, in contrast to the papers [14,17], the grid step ($h = L/N$) was 1 nm, which allowed to eliminate the occurrence of artifacts when performing calculations of MBL with nanometer-thick GaAs inserts and multilayer HEMT heterostructures, as well as to improve the accuracy of the calculations. The iterative process of calculation was stopped when the accuracy of determining the MD density was $50\,cm^{-2}$.

3. Results and discussion

Previously, we theoretically [14] and experimentally [18,19] studied the nature and features of the distribution of MD and elastic stresses in MBL $In_xAl_{1-x}As$ with a root profile of composition change depending on the final content of In (x_{max}). Meanwhile, the question of the influence of the initial composition of MBL (x_{min}) on its properties has not yet been studied in detail, and the values of x_{min} used in various papers [20,21] vary in a wide range, 0.05−0.15.

In the present work, the effect of the value of x_{min} in MBL $In_xAl_{1-x}As$ with a root profile on the density of the MD and the thickness of the dislocation-free region (d_{free}) in its upper part was studied on the theoretical basis. To do this, using the numerical method presented in Section 2, the calculations of the equilibrium distribution of the MD density along the growth axis were carried out for two series of MBL $In_xAl_{1-x}As$ with different initial contents of In ($x_{min} = 0.05-0.25$) and differing in the type of root profile of composition change (Fig. 1).

The profiles of changes in the MBL composition of the first series were dependences of the$x(z) = x_{min} + (x_{max} - x_{min})(z/L)^{1/2}$ form, where the final composition (x_{max}) and thickness (L) of the MBL remained unchanged and equal to 0.79 and 950 nm, respectively. The profiles of changes in the MBL composition of the second series were obtained from the dependence $x(z) = x_{min} + (x_{max} - x_{min})(z/L)^{1/2}$, where $x_{min} = 0.05$, $x_{max} = 0.79$, $L = 950$ nm, by cutting off the lower part (reducing the thickness) of the MBL to the required minimum composition of x_{min}. The results of calculations for the MBL of the first and second series are shown in Fig. 1, *a* and *b*, respectively. The inserts show to the figures the dependences of the MD density in the upper part of the MBL (ρ_{end}) and the thickness of the dislocation-free area (d_{free}) of the value of x_{min}. It can be seen that in MBL of the first series, as x_{min} is increased from 0.05 to 0.25, ρ_{end} decreases by a factor of 1.4, while d_{free} increases insignificantly from 100 to 120 nm. In MBL of the second series, with an increase in x_{min}, the value of d_{free} increases twice and ρ_{end} increases in contrast to the first series, which, apparently, is explained by a decrease in the thickness of the MBL. Meanwhile, the increase in the thickness of d_{free} with

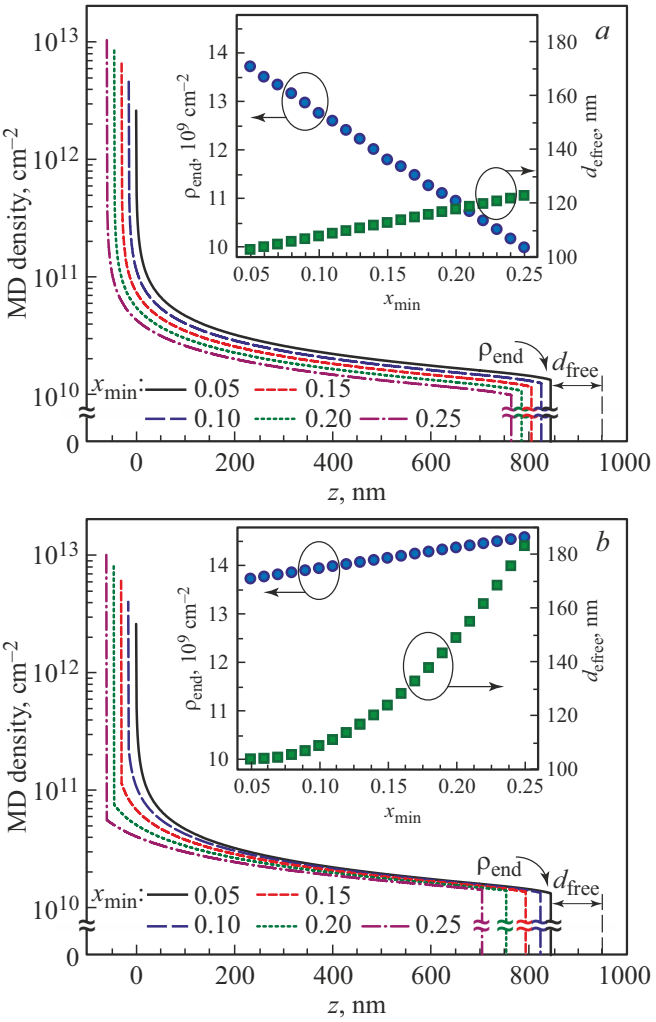

Figure 1. Equilibrium MD density distribution along the growth axis for two series of MBL $In_xAl_{1-x}As$/GaAs with different initial content of In$x_{min} = 0.05-0.25$and differing in the form of the root profile of the composition change: *a* — $x(z) = x_{min} + (x_{max} - x_{min})(z/L)^{1/2}$, where $x_{max} = 0.79$, $L = 950$ nm — the final composition and thickness of the MBL, respectively; *b* — obtained from the profile $x(z) = x_{min} + (x_{max} - x_{min})(z/L)^{1/2}$, where $x_{min} = 0.05$, $x_{max} = 0.79$, $L = 950$ nm, by cutting off the lower part of the MBL to the required value x_{min}. The calculated dependencies are shifted relative to each other by 15 nm for ease of perception. The inserts show — dependences of the MD density in the upper part of the MBL (ρ_{end}) and the thickness of the dislocation-free area (d_{free}) on the initial composition of x_{min}.

an increase in x_{min} in MBL of the second series occurs nonlinearly and, at values of $x_{min} > 0.15$, is much faster than in the first series.

Thus, the minimum calculated MD density ($\rho_{end} \sim 9.9 \cdot 10^9$ cm^{-2}), preceding the dislocation-free area, is achieved in the MBL of the first series when using the maximum initial content In $x_{min} = 0.25$. This is explained by the fact that in the first series, at a constant MBS thickness, the use of large values of x_{min} allows to make the transition to the final $x_{max} = 0.79$ composition smoother. It should be noted that the values of $x_{min} > 0.25$ were not considered, since the growth of such MBL sharply increases the probability of the transition of the epitaxial growth mode from layer-by-layer (two-dimensional) to three-dimensional.

An important task in the creation of metamorphic heterostructures is also the reduction of the TD density, which correlates with the MD density [22]. One of the approaches leading to a decrease in the density of TD in metamorphic structures is the use of single elastically stressed layers in MBL, which allow to change the direction of TD propagation up to their bending in the growth plane. The effectiveness of this approach was first demonstrated using the GaN/AlN [23] system as an example, and was also experimentally confirmed for the (In,Ga,Al)(As,Sb) [24] system. However, due to the lack of a complete theory of relaxation of elastic stresses for MBL with an arbitrary composition change profile, the problem of optimizing the thicknesses of elastically stressed layers and their positions in MBL remains relevant today.

In this work, the nature of the distribution of MD along the growth axis of the $In_xAl_{1-x}As$ MBL with a root profile of the change in the composition was studied depending on the thickness and position of elastically stretched GaAs layers in the MBL. Fig. 2, *a* shows the results of calculations of the equilibrium distribution of the MD density along the growth axis for MBL $In_xAl_{1-x}As$ containing a GaAs insert of various thicknesses of 1–10 nm upon reaching the composition of $x \sim 0.39$ ($z = 200$ nm). From Fig. 2, *a* it can be seen that, regardless of the thickness of the GaAs insert, a dislocation-free area is formed under it, characterized by the thickness d_{free}^{GaAs} and similar to that formed in the upper part of the MBL. Meanwhile, with an increase in the thickness of the insert from 1 to 10 nm, the value of d_{free}^{GaAs}increases from 43 to 97 nm, and the MD density in the MBL area immediately after the insert (ρ_{GaAs}) increases from $1.5 \cdot 10^{12}$ to $3.6 \cdot 10^{12}$ cm^{-2} (see Table 1). Let us note that the formation of a dislocation-free area in the „root" MBL $In_xAl_{1-x}As$ was found earlier experimentally in the study of such structures using the method of transmission electron microscopy in the geometry of the cross section [24], and the calculated value $d_{free}^{GaAs} = 74$ nm in the case of a GaAs insert with a thickness of 5 nm correlates well with the corresponding experimental one (75–97 nm).

Table 1. Values of ρ_{GaAs} and d_{free}^{GaAs} at different thicknesses of the GaAs insert located in the MBL $In_xAl_{1-x}As$ with the root profile of composition change at $x \sim 0.39$ ($z = 200$ nm)

Thickness of the insert GaAs, nm	ρ_{GaAs}, cm^{-2}	d_{free}^{GaAs}, nm
1	$1.5 \cdot 10^{12}$	43
5	$2.6 \cdot 10^{12}$	74
10	$3.6 \cdot 10^{12}$	97

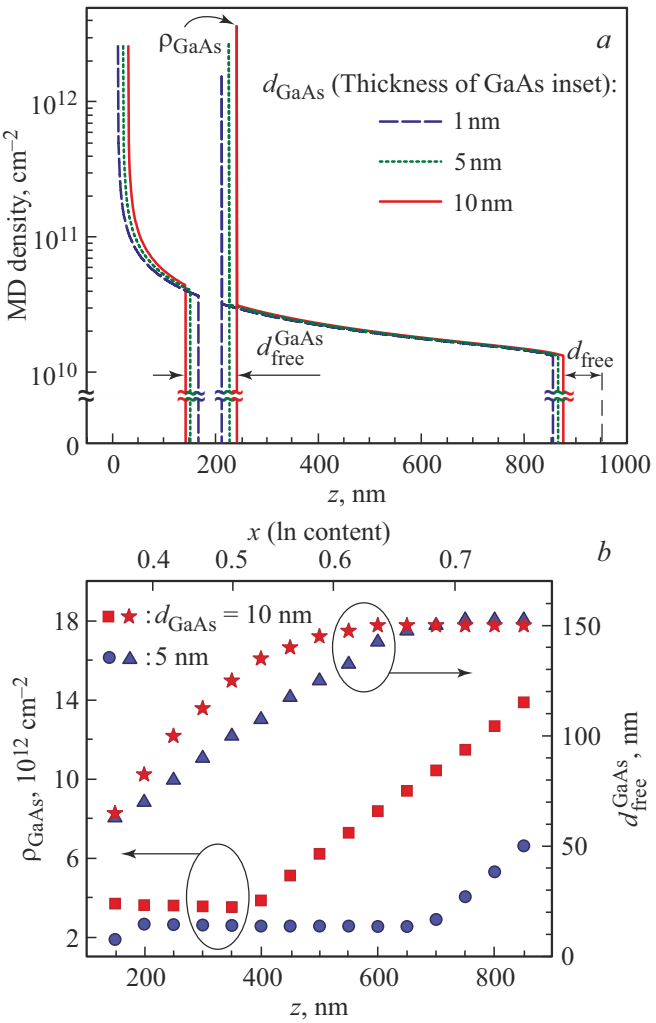

Figure 2. *a* — equilibrium density distributions of MD along the growth axis of MBL $In_xAl_{1-x}As$ with a root profile of composition change containing a single elastically stressed GaAs insert of various thicknesses 1–10 nm upon reaching the composition $x \sim 0.39$ ($z = 200$ nm). The calculated dependencies are shifted relative to each other by 10 nm for ease of perception; *b* — dependences of the thickness of the dislocation-free area (d_{free}^{GaAs}) located under the GaAs insert, as well as the MD density in the MBL area immediately after the GaAs insert (ρ_{GaAs}) on its position.

Fig. 2, *b* shows the dependences of ρ_{GaAs} and d_{free}^{GaAs} on the position of a 5 and 10 nm thick GaAs insert in the $In_xAl_{1-x}As$ MBL with a root profile of composition change. The influence of the position of the GaAs insert with a thickness of 1 nm on the values of ρ_{GaAs} and d_{free}^{GaAs} was not studied, since it was previously experimentally shown that MBL containing GaAs inserts with a thickness of 1 nm practically did not differ in their structural properties from MBL without an insert [24]. In case of 5 and 10 nm thick GaAs inserts, it can be seen from Fig. 2 *b* that the dependence $d_{free}^{GaAs}(z)$ first increases, and then, at $z \sim 650$ nm, saturates. Meanwhile, the value of the MD density in the MBL area immediately behind the ρ_{GaAs} insert remains constant when the insert position is changed to the values $z \sim 700$ and 400 nm for inserts with a thickness of 5 and 10 nm, respectively, and then, at higher values z, a sharp the increase in ρ_{GaAs}, apparently due to the relaxation of elastic stresses in the insert itself.

We have previously shown that a significant decrease in the near-surface dislocation density in MBL with a root profile of composition change over thickness compared to the case of „linear“ MBL is due to the fact that „root“ MBL is characterized by a rapid change in composition in the lower region, adjacent to the GaAs substrate, and smooth — in its upper part [16]. In addition, such an MBL profile leads to a decrease in the disorder of the solid solution in the area of high compositions [15]. In order to search for a profile shape that would lead to a lower defect density, we calculated the MD density distribution along the growth axis for MBL $In_xAl_{1-x}As$ with various nonlinear profiles of composition change of the form $x(z) = x_{min} + (x_{max} - x_{min})(z/L)^{1/n}$, where L — the thickness of the MBL equal to 950 nm, x_{min} and x_{max} — initial and final content of In in MBL, equal to 0.05 and 0.79, respectively, and n — natural number from 2 to 5 (Fig. 3).

As can be seen from the insert in Fig. 3, with an increase in n, the steepness of the composition change profile in the initial section increases and, accordingly, decreases in the final section, which should lead to a decrease in the MD density. Indeed, the simulation results showed that the lowest MD density (ρ_{end}), as well as the largest thickness of the dislocation-free area (d_{free}) is achieved in MBL with the highest value n (see Fig. 3 and Table 2).

Nevertheless, the technological implementation of such MBL with $n > 2$ is difficult due to a sharp change in the composition in the first tens of nanometers (see insert in Fig. 3). To solve this problem, a profile (see formula (2)) is proposed, the initial part of which is determined by the root dependence $\propto z^{1/2}$, and the final part by the power dependence $\propto z^{1/n}$ with the maximum n

$$x(z) = x_{min} + (x_{max} - x_{min}) \times \left(\frac{(L-z)\left(\frac{z}{L}\right)^{1/2} + z \cdot \lim\limits_{n\to\infty} \left(\frac{z}{L}\right)^{1/n}}{L} \right). \quad (2)$$

Simplifying formula (2), we obtain the final expression for the optimized profile of the change in the MBL composition $In_xAl_{1-x}As$: $x(z) = x_{min} + (x_{max} - x_{min}) \times \left((z/L)^{1/2} + (z/L) - (z/L)^{3/2}\right)$. For MBL with such a profile, we also calculated the equilibrium density distribution of MD along the growth axis and found that an MBL with an optimized nonlinear composition change profile allows to reduce the density of near-surface MD (ρ_{end}) in ~ 2.2 by times, and also to double the thickness of the dislocation-free area (d_{free}) compared to „root“ MBL (see Table 2).

To understand the influence of the MBL design on the features of elastic stress relaxation directly in metamorphic

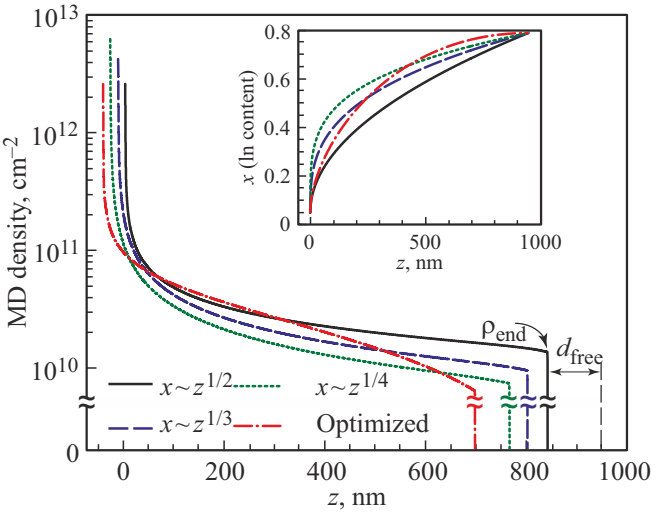

Figure 3. Equilibrium distribution of MD density along the growth axis for MBL $In_xAl_{1-x}As$ with different nonlinear composition change profiles of the $x(z) \propto z^{1/n}$ type and optimized profile $x(z) = x_{min} + (x_{max} - x_{min})\left((z/L)^{1/2} + (z/L) - (z/L)^{3/2}\right)$. The calculated dependencies are shifted relative to each other by 15 nm for ease of perception. The insert shows the corresponding profiles of changes in the MBL composition.

heterostructures, the calculations of the equilibrium distribution of the MD density over the thickness of two m HEMT heterostructures (structures A and B) were carried out, which differ only in the MBL design. Structures A and B included MBL $In_xAl_{1-x}As$ with a root ($x \propto z^{1/2}$) and an optimized nonlinear profile of the change in the composition (see formula (2)), respectively. The following sequence of layers typical of HEMT heterostructures (Fig. 4, a) was used in the calculations: GaAs substrate, MBL $In_xAl_{1-x}As$ (950 nm), lower barrier layer $In_{0.75}Al_{0.25}As$ (virtual substrate — VS) 40 nm thick, quantum well $In_{0.75}Ga_{0.25}As$ (24 nm), upper barrier layer $In_{0.75}Al_{0.25}As$ (84 nm) and cover layer $In_{0.75}Ga_{0.25}As$ (4 nm). The value of the inverse step was varied within$\Delta = 0.02-0.14$ by corresponding changes in the final content of In in MBL (x_{max}). It was found that in the A structure, when the $\Delta < 0.10$ value is used, the relaxation of elastic mechanical stresses occurs exclusively inside the MBL, while the active layers of the m HEMT structure are completely absent (see insert in Fig. 4, b). At the same time, at values of the reciprocal step $\Delta \geq 0.10$, relaxation of elastic stresses at the MBL/virtual substrate interface is observed (Fig. 4, b). It should be noted that the calculated results agree fairly well with the experimental data. For example, we have previously shown that in the case of optical metamorphic In(As,Sb)/In(Ga,Al)As heterostructures obtained by molecular beam epitaxy on GaAs substrates and containing InAlAs MBL with a root profile of composition change, the maximum the value of the internal quantum efficiency was achieved at $\Delta = 0.08-0.10$ [18,19].

Meanwhile, in the In(As,Sb)/In(Ga,Al)As structures with $\Delta \geq 0.12$, when they were studied by the method of transmission electron microscopy in the cross-sectional geometry, TDs nucleating at the MBL/virtual substrate interface [19]. In addition, the calculated value of the

Table 2. MD density (ρ_{end}) and thickness of the dislocation-free area (d_{free}) in the upper part of the MBL $In_xAl_{1-x}As$ with different nonlinear composition change profiles ($x_{min} = 0.05$, $x_{max} = 0.79$, $L = 950$ nm)

Profile of composition change of $x(z)$ MBS $In_xAl_{1-x}As$	ρ_{end}, cm^{-2}	d_{free}, nm
$x_{min} + (x_{max} - x_{min})(z/L)^{1/2}$	$1.4 \cdot 10^{10}$	104
$x_{min} + (x_{max} - x_{min})(z/L)^{1/3}$	$9.3 \cdot 10^{9}$	129
$x_{min} + (x_{max} - x_{min})(z/L)^{1/4}$	$7.2 \cdot 10^{9}$	150
$x_{min} + (x_{max} - x_{min})(z/L)^{1/5}$	$5.9 \cdot 10^{9}$	167
$x_{min} + (x_{max} - x_{min}) \times \left((z/L)^{1/2} + (z/L) - (z/L)^{3/2}\right)$	$6.2 \cdot 10^{9}$	204

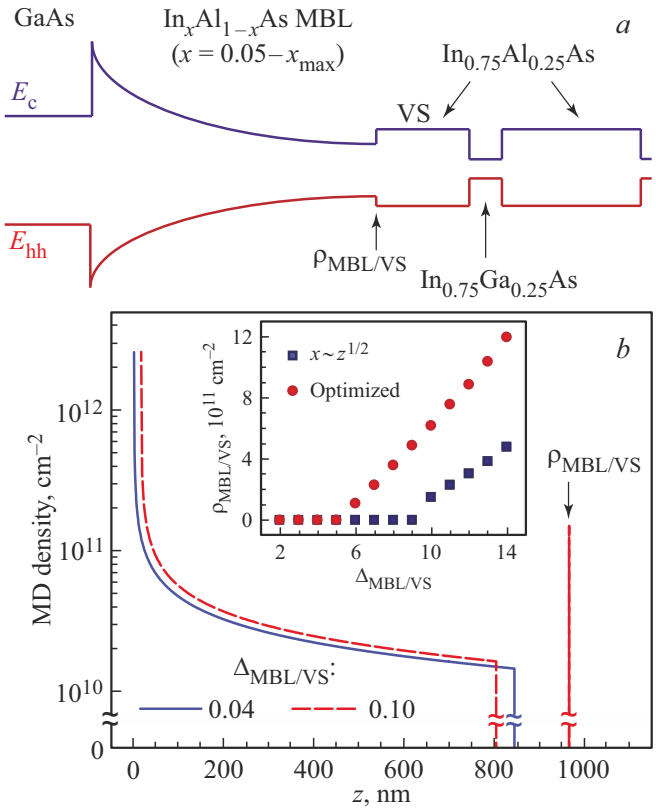

Figure 4. a — Schematic band diagram of a metamorphic HEMT heterostructure including an MBL $In_xAl_{1-x}As$ with a nonlinear profile of composition change, a virtual substrate (VS) $In_{0.75}Al_{0.25}As$, and a two-dimensional electronic channel $In_{0.75}Ga_{0.25}As/In_{0.75}Al_{0.25}As$; b — equilibrium distributions of the MD density along the structure growth axis A with different reciprocal steps $\Delta = 0.04$ and 0.10. The calculated dependencies are shifted relative to each other by 15 nm for ease of perception. The insert shows the MD densities at the MBL/virtual substrate interface depending on the value of the inverse step for structures A and B.

thickness of the dislocation-free region in the upper part of the MBL $d_{\text{free}} = 103$ nm for the A structure with $\Delta = 0.04$ agree fairly well with the experimental value determined by the method of local electron diffraction from a selected region (~ 110 nm) [25]. It should be noted that the use of MBL in the *m* HEMT heterostructure with a nonlinear optimized composition change profile (structure B) leads to the fact that the relaxation of elastic stresses with the formation of MD at the MBL/virtual substrate interface occurs at much lower values of the inverse step $\Delta \geq 0.06$ (see inset in Fig. 4, *b*).

It seems of interest to estimate the TD density in heterostructures containing MBL with a non-linear optimized profile of composition change. Previously, it was shown that an MBL with a root profile of composition changes allows to reduce the MD density in its upper part by a factor of ~ 2 times compared to an MBL with a linear profile [14]. Meanwhile, it was experimentally shown that the TD density, which correlates with the MD density, in structures containing MBL with a root profile is 3 times less than in structures containing „linear" MBL, and is $(5 \pm 2) \cdot 10^7$ cm $^{-2}$ [3]. Taking these facts into account, as well as the fact that the MBL proposed in this paper with an optimized nonlinear profile of composition change allows to reduce the density of MD by ~ 2.2 times compared with the „root" MBL, one should expect a decrease in the TD density in structures containing MBL with an optimized profile, up to $\sim 10^7$ cm^{-2}.

4. Conclusion

The calculations of the equilibrium distribution of the MD density along the growth axis were carried out for MBL $In_xAl_{1-x}As$ with different initial contents of In ($x_{\min} = 0.05-0.25$) and differing in the type of root profile of composition change. It has been established that the minimum calculated density of MD in the upper part of the MB is achieved in the case of $x_{\min} = 0.25$. The dependence of the MD distribution along the growth axis of the InAlAs MBL with a root profile of composition change on the thickness and position of single ultrathin (1–10 nm) elastically stressed GaAs layers in the MBL is studied. It is shown by numerical simulation that, regardless of the thickness of the GaAs insert, a dislocation-free area is formed under it, similar to the one that forms in the upper part of the MBL, and which was observed earlier experimentally. In this case, the value of the thickness of this area free from dislocations agrees fairly well with the experimental value obtained using transmission electron microscopy in the cross section geometry. The equilibrium density distribution of MD along the direction of epitaxial growth of MBL $In_xAl_{1-x}As/GaAs$ with the maximum content of In $x_{\max} \geq 0.77$ and various nonlinear profiles of composition change of the form $x \propto z^{1/n}$ were calculated. An optimized nonlinear profile of the composition change of the InAlAs MBL is proposed, which allows to obtain in its upper part a density of MD that is half that of the root profile. Calculations were made of the equilibrium density distribution of MD over the thickness of metamorphic HEMT heterostructures containing MBL $In_xAl_{1-x}As$ of various designs and a two-dimensional electron channel $In_{0.75}Ga_{0.25}As/In_{0.75}Al_{0.25}As$. In case of using MBL in HEMT structures with a root and an optimized profile of composition change, the values of the inverse step are set: $\Delta < 0.10$ and $\Delta < 0.06$ respectively, at which the relaxation of elastic stresses occurs exclusively in the MBL, and is completely absent in the active layers of *m* HEMT heterostructures. The TD density was estimated in heterostructures containing MBL with a non-linear optimized profile of composition change which allow to expect a decrease in TD in such structures to values 10^7 cm^{-2}.

Funding

M.Yu. Chernov thanks the Russian Science Foundation (grant No. 22-79-00265) for partial support of these studies.

Conflict of interest

The authors declare that they have no conflict of interest.

References

[1] S.H. Shin, J.-P. Shim, H. Jang, J.-H. Jang. Micromachines, **14** (1), 56 (2023).
[2] J. Ajayan, D. Nirmal. Superlat. Microstruct., **86**, 1 (2015).
[3] S.V. Ivanov, M.Yu. Chernov, V.A. Solov'ev, P.N. Brunkov, D.D. Firsov, O.S. Komkov. Progr. Cryst. Growth Charact. Mater., **65** (1), 20 (2019).
[4] S. Ke, D. Li, S. Chen. J. Phys. D: Appl. Phys., **53**, 323001 (2020).
[5] Y. Du, B. Xu, G. Wang, Y. Miao, B. Li, Z. Kong, Y. Dong, W. Wang, H.H. Radamson. Nanomaterials, **12** (5), 741 (2022).
[6] M.S. Abrahams, L.R. Wiesberg, C.J. Buiocchi, J. Blanc. J. Mater. Sci., **4**, 223 (1969).
[7] J. Tersoff. Appl. Phys. Lett., **62**, 693 (1993).
[8] G.B. Galiev, S.S. Pushkarev, E.A. Klimov, P.P. Maltsev, R.M. Imamov, I.A. Subbotin. Crystallography Reports, **59**, 258 (2014).
[9] L.W. Khai, T.K. Hua, L. Daosheng, S. Wicaksono, Y.S. Fatt. IEEE Phot. Techn. Lett., **29** (5), 458 (2017).
[10] Y. He, W. Yan. Optical Quant. Electron., **52**, 372 (2020).
[11] S. Park, J. Jeon, V.M. More, R.S. Lee, Y. Seo, M. Kim, P.D. Nguyen, M. Kim, J.S. Kim, Y. Kim, S.J. Lee. Appl. Surf. Sci., **581**, 152421 (2022).
[12] D.J. Dunstan. J. Mater. Sci.: Mater. Electron., **8**, 337 (1997).
[13] F. Romanato, E. Napolitani, A. Carnera, A.V. Drigo, L. Lazzarini, G. Salviati, C. Ferrari, A. Bosacchi, S. Franchi. J. Appl. Phys., **86**, 4748 (1999).
[14] D.V. Pobat, V.A. Soloviev, M.Yu. Chernov, S.V. Ivanov. FTT, **63** (1), 85 (2021). (in Russian).
[15] H. Choi, Y. Jeong, J. Cho, M.H. Jeon. J. Cryst. Growth, **311** (4), 1091 (2009).

[16] M.Yu. Chernov, O.S. Komkov, D.D. Firsov, B.Ya. Meltser, A.N. Semenov, Ya.V. Terent'ev, P.N. Brunkov, A.A. Sitnikova, P.S. Kop'ev, S.V. Ivanov, V.A. Solov'ev. J. Cryst. Growth, **477**, 97 (2017).
[17] B. Bertoli, E.N. Suarez, J.E. Ayers, F.C. Jain. J. Appl. Phys., **106**, 073519 (2009).
[18] M.Yu. Chernov, V.A. Solov'ev, O.S. Komkov, D.D. Firsov, B.Ya. Meltser, M.A. Yagovkina, M.V. Baidakova, P.S. Kop'ev, S.V. Ivanov. Appl. Phys. Express, **10**, 121201 (2017).
[19] O.S. Komkov, D.D. Firsov, M.Yu. Chernov, V.A. Solov'ev, A.A. Sitnikova, P.S. Kop'ev, S.V. Ivanov. J. Phys. D: Appl. Phys., **51**, 055106 (2018).
[20] G.B. Galiev, S.S. Pushkarev, I.S. Vasil'evskii, E.A. Klimov, R.M. Imamov, I.A. Subbotin, E.S. Pavlenko, A.L. Kvanin. Crystallography Reports, **57**, 841 (2012).
[21] T. Ganbold, M. Antonelli, G. Biasiol, G. Cautero, H. Jark, D.M. Eichert, R. Cucini, R.H. Menk. J. Instrum., **9**, C12043 (2014).
[22] M. Tamura, A. Hashimoto, Y. Nakatsugawa. J. Appl. Phys., **72**, 3398 (1992).
[23] V.N. Jmerik, D.V. Nechaev, S. Rouvimov, V.V. Ratnikov, P.S. Kop'ev, M.V. Rzheutski, E.V. Lutsenko, G.P. Yablonskii, M. Aljohenii, A. Aljerwii, A. Alyamani, S.V. Ivanov. J. Mater. Res., **30**, 2871 (2015).
[24] V.A. Soloviev, M.Yu. Chernov, O.S. Komkov, D.D. Firsov, A.A. Sitnikova, S.V. Ivanov. Pisma ZhETF, **109** (6), 381 (2019). (in Russian).
[25] V.A. Solov'ev, M.Yu. Chernov, M.V. Baidakova, D.A. Kirilenko, M.A. Yagovkina, A.A. Sitnikova, T.A. Komissarova, P.S. Kop'ev, S.V. Ivanov. Superlat. Microstruct., **113**, 777 (2018).

Translated by E.Potapova